1282 *Chem. Mater.* **2010,** *22,* 1282–1284
DOI:10.1021/cm903105f

CHEMISTRY OF MATERIALS
Communication

Solution-Based Epitaxial Growth of Magnetically Responsive Cu@Ni Nanowires

Shengmao Zhang[†,‡] and Hua Chun Zeng*[,†]

[†]*Department of Chemical and Biomolecular Engineering and KAUST-NUS GCR Program, Faculty of Engineering, National University of Singapore, 10 Kent Ridge Crescent, Singapore 119260, and* [‡]*The Key Laboratory of Ministry of Education for Special Functional Materials, Henan University, Kaifeng 475004, China*

Received October 7, 2009
Revised Manuscript Received January 8, 2010

Over the past decade, one-dimensional (1D) nanomaterials have attracted significant interest because of their important applications in the fields of electronics, devices, composites, catalysis, and sensing.[1−16] For instance, core/shell or coaxial nanowires are now a class of 1D nanostructures under extensive investigation. There have been many types of combinations for these composite nanowires, ranging from metal/metal,[3−5] semiconductor/semiconductor,[6−11] metal/semiconductor,[12,13] to inorganic/organic or organic/inorganic, etc.[14,15] In this connection, a number of preparative methods, such as electrodeposition,[3,4] chemical vapor deposition,[6,7,12] atomic layer deposition,[9] pulsed laser deposition,[10,11] thermal evaporation,[13] solution-based chemical methods, etc.,[5,8,15,16] have been developed. Nevertheless, most of these methods involve two or more processing steps, and catalysts and/or templates are commonly required, especially in the synthesis of preformed core-nanowires. To the best of our knowledge, there has been no report so far on "one-pot" synthesis of core/shell coaxial metal nanowires without using templates. Herein we select metallic copper (Cu) as a core material in our exploration of one-pot synthesis of 1D core/shells, as copper is an ideal interconnecting material for micro- and nanoelectronics.[1,2,16] More importantly, we also introduce ferromagnetic nickel (Ni) as an overcoat material to the copper, which makes diamagnetic Cu nanowires become magnetically guidable for self-assembly.

The Ni-sheathed Cu nanowires (Cu@Ni nanowires) were synthesized with a one-pot approach. In a typical synthesis, 30 mL of high concentration NaOH (7.0 M), 0.1−1.0 mL of $Cu(NO_3)_2 \cdot 3H_2O$ (0.1 M), or 0.07−0.20 mL of $Cu(NO_3)_2 \cdot 3H_2O$ (0.5 M) and 0.07−0.30 mL of $Ni(NO_3)_2 \cdot 6H_2O$ (0.5 M) aqueous solutions were added into a plastic reactor with a capacity of 50.0 mL. A varying amount of ethylenediamine (EDA; 0.15−0.50 mL; 99 wt %) and hydrazine ($N_2H_4 \cdot H_2O$, 0.025−0.20 mL; 80 wt %) were also added sequentially, followed by thorough mixing of all reagents. Synthetic reactions were carried out at 80 °C for 1 h, after which the reactor was cooled naturally in laboratory air. The products were washed and harvested with centrifugation−redispersion cycles. Further details on the synthesis can be found in the Supporting Information (SI-1). The crystallographic phases of the as-prepared metallic nanowires were investigated using powder X-ray diffraction method (XRD, Shimadzu XRD-6000, Cu K_α radiation, λ = 1.5406 Å) at a scanning rate of 2°/min. The dimension, morphology, and chemical composition of the products were examined with scanning electron microscopy with energy dispersive X-ray spectroscopy (SEM/EDX; JSM-5600LV), transmission electron microscopy (TEM/EDX, JEM-2010, 200 kV), high-resolution TEM and selected area electron diffraction (HRTEM/SAED/EDX, JEM-2100F, 200 kV) with EM-24015 scanning image observation device, inductively coupled plasma (ICP; Perkin-Elmer Optima 2100 DV) spectroscopy, and X-ray photoelectron spectroscopy (XPS; AXIS-HSi, Kratos Analytical). Magnetic properties of the nickel phase in Cu@Ni nanowires were studied using superconducting quantum interference device magnetometry (SQUID; Quantum Design Inc., MPMSXL-5) over a temperature range of 5 to 300 K and a magnetic field strength of 0 to 30 kOe; zero-field-cooling (ZFC) and field-cooling (FC, at 100 Oe) measurements were also carried out.

Figure 1a shows a panoramic view of product morphology of Cu@Ni nanowires prepared with this "one-pot" approach. As can be seen, the nanowires are straight with constant diameters in the range of 200−300 nm (Figure 1b,c). The as-synthesized nanowires are very long, having lengths of more than several tens of micrometers. Importantly, the Cu core wires are sheathed with a Ni overcoat (Figure 1c) forming a coaxial cablelike

*Corresponding author. E-mail: chezhc@nus.edu.sg.

(1) Xia, Y.; Yang, P.; Sun, Y.; Wu, Y.; Mayers, B.; Gates, B.; Yin, Y.; Kim, F.; Yan, H. *Adv. Mater.* **2003**, *15*, 353−389, and references therein.
(2) Kuchibhatla, S. V. N. T.; Karakoti, A. S.; Bera, D.; Seal, S. *Prog. Mater. Sci.* **2007**, *52*, 699−913, and references therein.
(3) Wang, H.; Xu, C.; Cheng, F.; Zhang, M.; Wang, S.; Jiang, S. P. *Electrochem. Commun.* **2008**, *10*, 1575–1578.
(4) Liu, Z.; Elbert, D.; Chien, C. L.; Searson, P. C. *Nano Lett.* **2008**, *8*, 2166–2170.
(5) Zhang, G.; Wang, W.; Li, X. *Adv. Mater.* **2008**, *20*, 3654–3656.
(6) Hua, B.; Motohisa, J.; Kobayashi, Y.; Hara, S.; Fukui, T. *Nano Lett.* **2009**, *9*, 112–116.
(7) Goldthorpe, I. A.; Marshall, A. F.; Mclntyre, P. C. *Nano Lett.* **2008**, *8*, 4081–4086.
(8) Godbl, J. A.; Black, R. W.; Puthussery, J.; Giblin, J.; Kosel, T. H.; Kuno, M. *J. Am. Chem. Soc.* **2008**, *130*, 14822–14833.
(9) Hwang, Y. J.; Boukai, A.; Yang, P. *Nano Lett.* **2009**, *9*, 410–415.
(10) Wang, K.; Chen, J.; Zhou, W.; Zhang, Y.; Yan, Y.; Pern, J.; Mascarenhas, A. *Adv. Mater.* **2008**, *20*, 3248–3253.
(11) Hayden, O.; Greytak, A. B.; Bell, D. C. *Adv. Mater.* **2005**, *17*, 701–704.
(12) Gautam, U. K.; Fang, X.; Bando, Y.; Zhan, J.; Golberg, D. *ACS Nano* **2008**, *2*, 1015–1021.
(13) Ghoshal, T.; Biswas, S.; Kar, S. *J. Phys. Chem. C* **2008**, *112*, 20138–20142.
(14) Ko, H.; Lee, J.; Schubert, B. E.; Chueh, Y.-L.; Leu, P. W.; Fearing, R. S.; Javey, A. *Nano Lett.* **2009**, *9*, 2054–2058.
(15) Song, X.; Lei, J.; Li, Z.; Li, S.; Wang, C. *Mater. Lett.* **2008**, *62*, 2681–2684.
(16) Chang, Y.; Lye, M. L.; Zeng, H. C. *Langmuir* **2005**, *21*, 3746–3748.

 Published on Web 01/22/2010

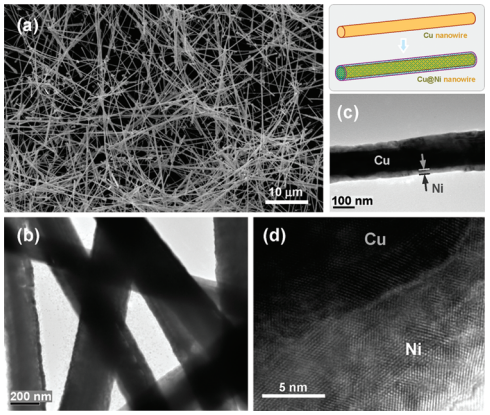

Figure 1. As-prepared Cu@Ni nanowires at different magnifications: (a) SEM image, (b, c) TEM images, and (d) HRTEM image. Color inset illustrates the deposition of Ni on in situ formed Cu nanowires.

structure with an overlayer thickness in the range of 20−30 nm. On the basis of the observed configuration, it is known that there must be a staged generation of the two transition metals in this synthetic route. Illustrated in the inset of Figure 1, the central Cu core is first formed, followed by a deposition of Ni sheath. More importantly, both the Cu cores and deposited Ni are essentially single-crystalline, as revealed by our HRTEM investigation (Figure 1d and SAED result which will be reported shortly). In particular, the metal overcoat (Ni) shows an epitaxial extension from the copper substrate although the lattice fringes in the interfacial regions (Figure 1d) are not exactly matched due to difference in lattice constants in the two face-centered cubic (fcc) transition metals (Cu: space group $Fm\bar{3}m$; $a_o = 3.615$ Å; JCPDS file No. 89−2838. Ni: space group $Fm\bar{3}m$; $a_o = 3.523$ Å; JCPDS file No. 87−0712).

To confirm the composite nature of Cu@Ni nanowires, XRD patterns, EDX line analysis and chemical mappings of our prepared samples were obtained. In Figure 2a, we report a progressive generation of the two transition metals. The Cu phase was formed after a reaction time of 25 min, and the nickel phase was observed 20 min later. Two sets of major diffraction peaks of (111), (200), and (220) are well-resolved, confirming that both metals have the same fcc crystal system. Across the radial direction of a Cu@Ni nanowire (see the dashed line in Figure 2b), $K_{\alpha 1}$ elemental line profiles clearly indicate that copper element has a maximum value in the center whereas the nickel has two maxima on both sides of this binary nanocomposite; the sheathed structure in the Cu@Ni nanowires is thus established. Furthermore, chemical mapping images of the two metal elements in the nanowire also draw the identical structural information (Figure 2b).

Because they have similar lattice parameters, copper and nickel are generally thought to exhibit solid solubility across the whole compositional range.[17] For instance, Cu−Ni alloy and composite nanocrystallites have been prepared, respectively, by reduction Ni^{2+} and Cu^{2+} with

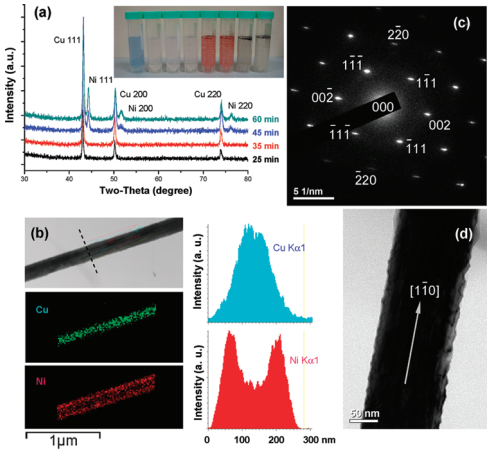

Figure 2. Characterization of Cu@Ni nanowires: (a) XRD pattern evolution of solid products, (b) lined EDX profiles and chemical mappings, (c) SAED pattern of a Cu@Ni nanowire, and (d) the nanowire that shows SAED pattern in (c). Color photo indicates product solutions/suspensions after different reaction times (left to right: 0, 5, 10, 15, 25, 35, 45, and 60 min).

N_2H_4 using water-in-oil microemulsion technique.[18] It has been found that the composition and size of Cu−Ni alloy or composite nanoparticles depend on the mole ratio of H_2O to sodium dodecyl sulfate, the method of addition of Cu^{2+} and Ni^{2+}, and the mole ratio of Cu^{2+} and Ni^{2+} in the initial precursor solution.[18] In our present synthesis, a strong basic condition was adopted, and the formation of the two metallic transition metals depends on the following redox reactions:

$$2Cu^{2+} + N_2H_4 + 4OH^- \rightarrow 2Cu + N_2 + 4H_2O \quad (1)$$

$$2Ni^{2+} + N_2H_4 + 4OH^- \rightarrow 2Ni + N_2 + 4H_2O \quad (2)$$

The standard reduction potential of copper [$E^o(Cu^{2+}/Cu^o) = +0.337$ V] is higher than that of nickel [$E^o(Ni^{2+}/Ni^o) = -0.257$ V], and copper is thus easier to be reduced in competitive redox reactions. On the basis of our present observation, it is thought that the copper complexes are more reducible toward hydrazine, since the copper phase is formed before the nickel under the identical conditions. According to coordination chemistry of the two transition metals, complexes such as $Cu(OH)_4^{2-}$ and $Cu(EDA)_2^{2+}$ are expected to be present in solution precursors, together with $Ni(EDA)_3^{2+}$ (which is less reducible).[16,19] Consistent with this analysis, the color change of the product solution shows a blue-purple ($Cu(OH)_4^{2-}$, $Cu(EDA)_2^{2+}$, and $Ni(EDA)_3^{2+}$) to light purple (in which $Ni(EDA)_3^{2+}$ was left, whereas blue-colored copper complexes were reduced to metallic nuclei), to radish brown (Cu nanowires), and to black (Cu@Ni nanowires) transformation upon the time (color photo of Figure 2). Our XPS analysis on the as-formed Cu nanowires confirms that there is indeed no nickel inclusion in the nanowires prior to the formation of nickel overcoat (see the Supporting Information, SI-2), which rules out the possibility of Cu−Ni alloy formation. It should also be mentioned that the reductive

(17) Cullity, B. D.; Graham, C. D. *Introduction to Magnetic Materials*, 2nd Ed.; Wiley-IEEE: New York, 2008.
(18) Feng, J.; Zhang, C.-P. *J. Colloid Interface Sci.* **2006**, *293*, 414–420.
(19) Zhang, S.; Zeng, H. C. *Chem. Mater.* **2009**, *21*, 871–883.

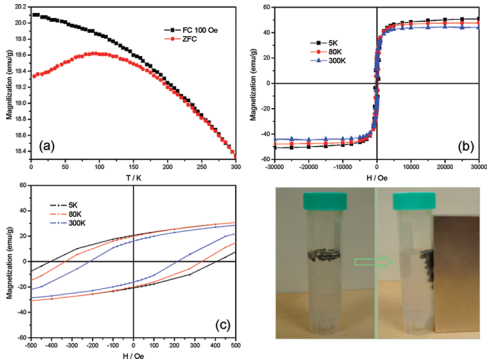

Figure 3. Magnetic characterization of as-prepared Cu@Ni nanowires: (a) magnetizations measured with field cooling (FC, 100 Oe) and zero-field cooling (ZFC) methods, (b) hysteretic loops at different temperatures, and (c) the central part of b. Color photos illustrate a responsive process of the nanowires to an external magetic bar.

conversion of Cu^{2+} and Ni^{2+} to metallic copper and nickel in this synthetic route is about 100%, which was indicated by decoloration of mother liquors (see color photos of Figure 3 later), ICP, and EDX analysis (see the Supporting Information, SI-1).

In Figure 2c,d, the SAED pattern of a Cu@Ni nanowire is displayed. Because the diffraction pattern can be assigned to [110] zone spots, the single-crystalline nature of the Cu core nanowires is affirmed despite unresolvable diffraction spots of the nickel overcoat. It appears that the growth of the Cu nanowire is along ⟨110⟩ directions, as copper atoms on the {110} crystal planes are coordinately less saturated, compared to other low Miller indexed crystal planes of {001} and {111}. Effects of experimental conditions on morphology of Cu@Ni products have also been examined. By varying different synthetic parameters and precursor ratios, for example, various product morphologies can be attained from prickly particles, prickly core/shell nanowires to smooth core/shell nanowires. Details for these additional controls over the nickel phase can be found in the Supporting Information, SI-3.

Temperature-dependent magnetization and hysteresis curves of the Cu@Ni nanowires were also measured, and analytical results are summarized in Table 1. In Figure 3a, the FC magnetization rises gradually when temperature decreases from 300 to 5 K, and it deviates from the ZFC curve at about 256 K (i.e., blocking temperature T_B) at which the ZFC and FC curves start to diverge. The relatively large T_B indicates that the as-synthesized nanowires possess appreciable ferromagnetic characteristics. In Figure 3b,c, the saturation magnetization (M_s) values of the sample at 5, 80, and 300 K are 50.9, 47.6, and 44.2 emu/g, respectively, which are quite similar to that of bulk nickel (~50−55 emu/g at room temperature), but significantly different from that of reported Ni nanoparticles.[20] On the other hand, the coercivity (H_c) values of the sample at 5, 80, and 300 K are 379.3, 331.3, and 237.2 Oe respectively, as presented in Figure 3c. Compared to the coercivity value of bulk nickel (0.7 Oe) and that of other 1D nanostructures of nickel, such as prickly Ni chains (88.9 Oe),[21] Ni nanowires (186.2 Oe),[22] Ni chains assembled by hollow microspheres (45 and 31 Oe)[23] and Ni nanofibers (124 Oe),[24] our Cu@Ni nanowires exhibit a significant enhancement in coercivity, which may be attributed to the formation of highly crystalline nickel overcoat with which coherent rotation of spins has to become a major fashion for the changes of magnetization, resulting in the observed larger coercivity. The observed enhancement in ferromagnetism of nickel and thus of Cu@Ni nanowires gives an important implication in self-assembly of Cu nanowires by the direction of magnetic field at room temperature. Interestingly, the as-prepared products tend to lift up to the top of solution because of their surface-adsorbed hydrophobic chelating agent. Indeed, the as-prepared Cu@Ni nanowires become mobile and response effectively to an external magnet, leaving colorless mother liquor behind. With the ferromagnetic Ni overcoat, the diamagnetic Cu nanowires can now be directed to a desired location under the guidance of external magnetic fields. Furthermore, nickel is more corrosion resistive, compared to copper. Therefore, the magnetically responsive Cu@Ni nanowires may find future applications in circuit/device fabrications using self-assembly approaches.[25]

Table 1. Analytical Results of Magnetic Properties of Nickel Phase in Cu@Ni Nanowires[a]

T (K)	M_s	H_c	M_r
5	50.9	379.3	20.6
80	47.6	331.3	19.6
300	44.2	237.2	15.7

[a] M_s = saturation magnetization of nickel (emu/g), H_c = coercivity (Oe), and M_r = remanence (emu/g); g is the unit weight of the nickel phase.

In summary, we have developed a simple solution-based epitaxial route to prepare nickel-sheathed copper nanowires under one-pot conditions. In particular, the nickel phase in the Cu@Ni nanowires exhibits a significant enhancement in coercivity at room temperature. With the new functionality provided by ferromagnetic nickel overcoat, diamagnetic copper nanowires become magnetically guidable with an applied magnetic field. These smart nanowires may serve as an ideal circuit-interconnect for self-assembled devices and circuit fabrications.

Acknowledgment. The authors gratefully acknowledge the financial support of the Ministry of Education, Singapore, and King Abdullah University of Science and Technology, Saudi Arabia.

Supporting Information Available: Experimental details, EDX, ICP, XPS and TEM results (PDF). This material is available free of charge via the Internet at http://pubs.acs.org.

(20) Wang, H.; Jiao, X.; Chen, D. *J. Phys. Chem. C* **2008**, *112*, 18793–18797.
(21) An, Z.; Pan, S.; Zhang, J. *J. Phys. Chem. C* **2009**, *113*, 1346–1351.
(22) Jia, F.; Zhang, L.; Shang, X.; Yang, Y. *Adv. Mater.* **2008**, *20*, 1050–1054.
(23) Wang, N.; Cao, X.; Kong, D.; Chen, W.; Guo, L.; Chen, C. *J. Phys. Chem. C* **2008**, *112*, 6613–6619.
(24) Wu, H.; Zhang, R.; Liu, X.; Lin, D.; Pan, W. *Chem. Mater.* **2007**, *19*, 3506–3511.
(25) Smith, P. A.; Nordquist, C. D.; Jackson, T. N.; Mayer, T. S.; Martin, B. R.; Mbindyo, J.; Mallouk, T. E. *Appl. Phys. Lett.* **2000**, *77*, 1399–1401.